JP&M Engineering
Journal of Petroleum and Mining Engineering

Effect of Infinite Volume on Structural Trapping Performance during Carbondioxide Sequestration Processes

Nyelebuchi Amadichuku,* Bright B. Kinate and Ayauwu A. Loveday
Depatment of Petroleum Engineering, Rivers State University, Nigeria
Corresponding author email: nyelebuchi.amadichuku@ust.edu.ng

Article Info

Received 28 Dec. 2023
Revised 12 Feb. 2024
Accepted 22 Mar. 2024

Keywords

CO_2 Sequestration; Structural trapping; infinite volume; pore volume;migration distance

Abstract

In this work, a compositional simulator (CMG-GEM) was employed to model the flow behavior of two components (CO_2 and H_2O) in the context of carbondioxide(CO_2) sequestration within a saline aquifer with infinite extent. A fluid model was built with the Peng Robinson EOS in a WINPROP and a base case model of limited extent aquifer with a range of volume modifiers assigned to boundary grid blocks as infinite was simulated. The amount of CO_2 trapped, its maximum migration distance, and CO_2 saturation distribution were analyzed for each of the aquifer volume considered.Pore volume modifiers of 10^3, 10^4, and 10^5 were sensitized. Results shows that saline aquifer of infinite extents complements the structural trapping of supercritical CO_2 by limiting the ultimate migration distance of CO_2 gravity currents. The quantity of trapped CO_2 exhibited a rise as the pore volume of the boundary blocks increased from 10^0 (base case) to 10^3, 10^4, and 10^5.For the base case,volume multiplier of 10^3, 10^4, and 10^5, the amount of CO_2 trapped were 59502925moles,88120568moles ,96803000moles, and 101404776moles showing an increase in moles as the volume increases. The base case model shows a CO_2 lateral migration distance of 525ft along the aquifer length while pore volume of 10^3, 10^4, and 10^5 gives a lateral migration distance of 884ft, 985ft and 985ft respectively. The results indicate that the infinite volume effects have caused a dispersed distribution of CO_2 trapped, contrasting with a concentrated distribution of mobile CO_2 in a limited aquifer.

Introduction

Since the onset of the industrial revolution, human activities and extensive use of fossil fuel energy have significantly increased the proportion of greenhouse gases in the atmosphere (Kelemen et al., 2019). This surge has resulted in environmental issues such as global warming, climate anomalies, and seawater acidification. Among various greenhouse gases like CO_2, N_2O, and CH_4, carbon dioxide (CO_2) exhibits the highest atmospheric concentration and can cause a robust greenhouse effect. Anthropogenic CO_2 emissions remain a critical driver of global climate change; hence efforts to mitigate their impact on Earth's climate have become paramount. Carbon capture, utilization, and storage encompass capturing carbon dioxide from its source of emission along with its associated compounds followed by compressing it for transportation before being utilized or permanently stored underground via injection into existing fields or geological formations (Ajayi et al., 2019: Yu et al., 2023). One promising method is carbon capture and storage (CCS), specifically underground sequestration of CO_2 in geological formations. In recent years CCS using CO_2 sequestration has emerged as a prominent solution to reduce greenhouse gas emissions (Kelemen et al., 2019).

Carbon dioxide (CO_2) sequestration involves injecting captured CO_2 into subsurface reservoirs, such as depleted oil and gas reservoirs, saline aquifers, or deep coal seams. Deep saline formations are abundant and provide safe long-term storage for permanent CO_2 immobilization. Once injected into geological storage formations, the CO_2 is rendered porous through various trapping mechanisms including structural or hydrodynamic trapping for caprocks and sedimentary formations; residual or capillary trapping prevalent in sedimentary formations; adsorption trapping dominant in organic-rich shale and coal seams; dissolution in brine and mineral trapping which are dominant mechanisms in basaltic and sedimentary formations.

The infinite volume effect estimates CO_2 storage capacity of underground formations theoretically infinite in size. This estimation is crucial to the oil and gas industry under increasing pressure to reduce greenhouse gas emissions while managing risk. While most other storage reservoirs have low CO_2 capacity, saline aquifers provide a viable destination for carbon sequestration with an estimated potential of several thousands of Giga Tons (Gt) of CO_2 (Wei et al., 2022).

However, filling this substantial capacity poses challenges due to injection-induced formation pressure increase that must remain below fracture pressure within limited drainage areas.

Studies undertaken by Anchliya (2009), Van Engelenburg (1993), Schembre-McCabe et al. (2007), Van der Meer and van Wees (2006), and Anchliya et al. (2012) revealed that the storage capacity of CO2 in a closed aquifer is significantly restricted due to reservoir pressurization during injection. The limitations arise from the incapacity of water to exit the system owing to compartmentalization, structural or stratigraphic constraints, and potential interference with other injection wells. Closed systems could be deemed effective for containing CO_2, benefitting from low-permeability barriers that deter CO_2 leakage. However, the limited capacity for CO_2 storage in these systems is attributed to the inability of displaced brine to escape. Extracting excess brine from the reservoir has the potential to alleviate heightened pressure, consequently augmenting the storage capacity of an aquifer for storing more CO_2 despite concerns over producing it from drainage wells. Open aquifers offer large storage potential with lower-pressure buildup making them desirable choices for CO_2 sequestration compared to their closed counterparts constrained by low-permeability barriers preventing leakage but limiting overall containment capability. Several authors have studied geologic sequestration options for infinite-sized aquifers as geological sequestration in closed ones is not feasible for managing carbon emissions. Van der Meet and Van Wees (2006) explored various aspects limiting pressure's impact on the potential storage capacity within finite saline aquifers.

Storage capacity is contingent upon the available space within specific geological formations; hence, injection well pressure will progressively grow with increasing volume accumulation when injecting more quantities into such formations. Thus maximum amount injected relies upon acceptable pressure increases without fracturing formations or moving existing faults; thus setting geomechanically determined thresholds above which pressures should not rise during operations could help manage them effectively.

Li et al (2014) and Buscheck et al (2012) demonstrated that proper placement methods can significantly enhance its management while reducing risks associated with breakthroughs at drainage sites during CO_2 injection and sequestration.

Guo et al.(2019) examined nanoparticle-stabilized foam's use to enhance megaporous saline aquifers' capacities while Han et al.(2023) investigation analyzed No 3 coal adsorption abilities within Qinshui Basin before assessing its geological capabilities as possible storages units for CO_2.

Ehlig-Economides and Economides (2010) argued against simulations assuming open-systems are secure alternatives to completely sealed lateral/vertical systems citing risk factors like diffuse/focused brine migration through sealing units causing bleed-offs leading towards semi-closed/open systems being better representatives than solely closed-system.

Amadichuku et al.(2023) provided data analysis regarding capillary-trapped gas saturation hysteresis impacts on maximum residual levels whereas upward migration unwantedly increases risks tied towards CO_2 leakage between surface-storage sites hence mitigation efforts target vertical migration reduction improvements increasing containment security/storage capacities.

Previous work indicates subsurface long-term CO_2 sequestering possibilities under ideal conditions but complex interplay between geological properties/fluid dynamics/sequestration process itself must be evaluated closely. It is important to understand the mechanisms governing trapped-CO_2 and form policy decisions optimizing carbon capture and storage (CCS) operations and contributing positively towards global climate change. Therefore, this work will evaluate the impact of infinite volume on structural trapping performance during Carbondioxide sequestration.

Materials and Methods

Materials

The materials, Software and input variables that are used includes: CMG pre-processor, Builder for creating GEM dataset, WINPROP fluid modelling program for GEM fluid model creation, GEM module of the CMG Builder software for model verification and simulation runs, Rock physics functions (relative permeability, porosity and saturations), grid properties data (grid dimensions in the x, y and z directions, permeability of the grid cells in x, y and z directions, grid thickness, number of grid cells in the x, y and z directions and depth to the top of reservoir), fluid properties data (compositional analysis, brine properties),well data (trajectory and constraint, well type, injection fluid and composition etc), gas relative permeability data, water relative permeability data, and model initialization data .They are presented in Table 1 - 5.

Table 1 Grid properties data

Properties	Value
Grid Top	1200m
Grid thickness	5m
Permeability (I, J and K)	100 millidarcies
Porosity	0.12
Rock compressibility	5.5e-7 per kPa
Reference pressure for rock compressibility	11800 kPa

Table 2 Data for GEM fluid model creation

Component	Mole fraction
CH4	0.999
CO_2	0.001
Reservoir temperature for GEM fluid model	50°C

Table 3 Water relative permeability data

Sw	krw	krow
0.2	0	1
0.2899	0.0022	0.6769
0.3778	0.018	0.4153
0.4667	0.0607	0.2178
0.5558	0.1438	0.0835
0.6444	0.2809	0.0123
0.7	0.4089	0
0.7333	0.4855	0
0.8222	0.7709	0
0.9111	0.95	0
1	0.9999	0

Table 4 Gas relative permeability data

Sg	krg	krog
0.0006	0	1
0.05	0	0.88
0.0889	0.001	0.7023
0.1778	0.01	0.4705
0.2667	0.03	0.2963
0.3556	0.05	0.1715
0.4444	0.1	0.0878
0.5333	0.2	0.037
0.6222	0.35	0.011
0.65	0.39	0
0.7111	0.56	0
0.8	0.9999	0

Table 5 Model initialization data

Properties	Value
Temperature	50°C
Reference pressure	11800 kPa
Datum depth	1200m
Water gas contact	1150m
CO_2fraction	0.001
CH_4	0.999

Methods

GEM, CMG's greenhouse gas simulator was used to create the base case aquifer model of finite volume (pore volume modifier = 1.0). The dataset was written using Builder and then verified using CMG-GEM, a 2D homogeneous aquifer model was established with block widths measuring 10 feet in both the x and y directions. This model featured dimensions were 100x1x20 (2000 grid blocks) in the x, y, and z directions. The data in Table 1 was used to fill the model with petrophysical, grid, and rock attributes. A compositional fluid model needed in the component portion of the CMG-GEM data file was generated using WINPROP. The fluid model was made up of supercritical CO_2 and CH_4 in proportions of 0.001 and 0.999 as presented in Table 2, with Peng Robinson model selected as the EoS for calculating thermodynamic properties. The CH_4 component was considered as the trace element to maintain a minimal volume in the aquifer, allowing for some compressibility in the system as residual gas. The created fluid model was incorporated into the component section of the GEM data file. The relative permeability curves were defined using the relative permeability data in Tables 3 and 4, and Table 5 data used to initialize the model. The model was completely saturated with brine as the water-gas interface or contact was placed at 1150 meters above the reference depth. Supercritical CO_2 fraction of 0.001 and CH_4 fraction of 0.999 were used to initiate the gas cap. At depths of 1298m, 1299m, and 1300m, a single injector well titled 'CO_2_INJECTOR' was placed at the base of the model across three levels. The injector well was used to inject pure supercritical CO_2 into the aquifer steadily for one year at a maximum surface gas rate of 10,000 m^3/day and a maximum BHP of 44,500 kPa. Subsequently, the simulation ran for an additional 199 years after the injector was shut-in, with the flow being solely driven by natural gradients and density variations.

After developing the base case model for a finite aquifer boundary, volume modifiers were employed to replicate an aquifer that features an open boundary, incorporating a significant portion of the aquifer beyond the simulation region. Pore volume multipliers were employed on the boundary blocks to establish a constant-pressure boundary. A number of simulation runs were conducted for three different cases with aquifer boundary block pore volume multipliers of 10^3, 10^4, and 10^5. The simulation workflow is presented in figure 1.

DOI: 10.21608/jpme.2024.258954.1185

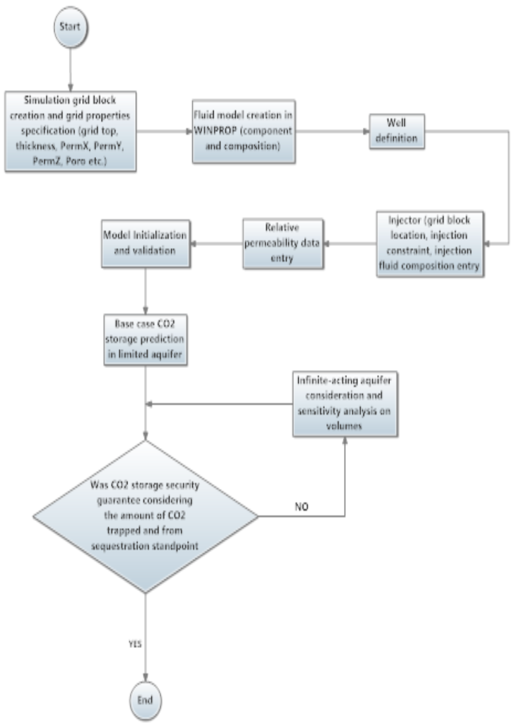

Figure 1 Simulation workflow

Results

Base case study for limited aquifer

Figure 2 depicts the CO_2 saturation distribution across the saline aquifer in the model's base case (closed aquifer boundary). In a limited aquifer, the base case model simulates a one-year CO_2 injection and the subsequent 199 years of CO_2 plume migration. During injection, the CO_2 moved laterally in the model due to the pressure created by the injection well, as illustrated in Figure 2.

Following injection, the plume's lateral growth stopped, and CO_2 moved upward because it had a lower density than formation water as shown in Figure 3.

The CO_2 plume moves upward owing to buoyancy forces with a little trail of residual saturation behind.

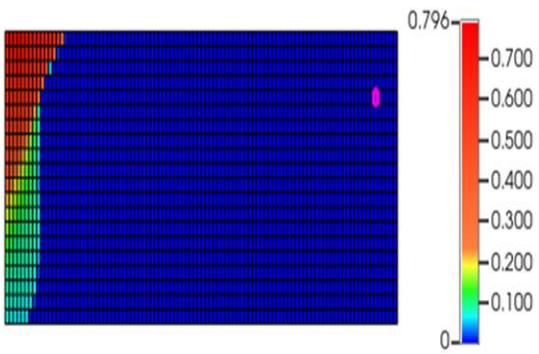

Figure 2 Upward movement of CO_2 plume owing to lighter density in limited aquifer

The model predicts that a high saturation of mobile CO_2 would emerge at the top of the formation after 199 years, which is a sufficiently long time as presented in Figure 3.Results further reveal that greater proportion of supercritical CO_2 occupies the first two layers of the structure. The gas saturation at the advancing front was 0.5218736 in grid block with address of 5311 at a distance of 525ft along the aquifer length.

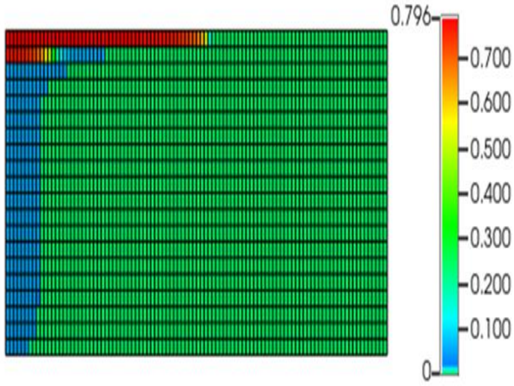

Figure 3 CO_2 saturation distribution at 200 years of injection

The quantity of trapped CO_2 after a 200-year period for the base case aquifer model with the boundary blocks having a default pore volume of 1.0 is shown in figure 4. Result shows that with a default pore volume of 1.0, the injection well's pressure induces movement, gradually trapping an increasing amount of CO_2 within the adjacent pore spaces as the injection period progresses. Throughout the injection period, 13,618,751 moles of CO_2 was initially trapped. Following injection, the trapped CO_2 notably escalates as the plume migrates upward due to natural buoyancy, reaching 59,502,924 moles over a span of 199 years.

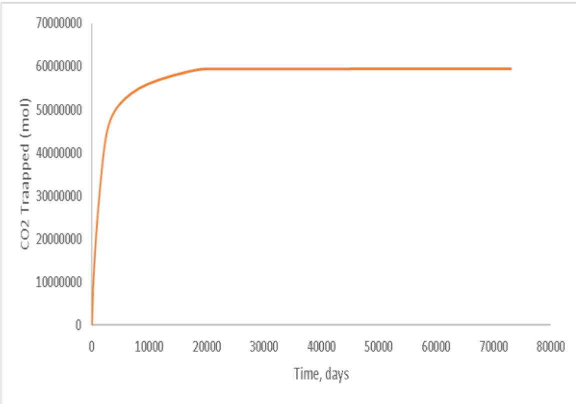

Figure 4 CO_2 Trapped for the base case study in finite volume aquifer.

Infinite volume effect

To simulate realistic aquifer conditions extending beyond the grid boundaries (open aquifer), a high pore volume multiplier was applied to the boundary blocks. In particular, these grid blocks' pore volume was multiplied by a factor of 103, 104 and 105. This method has worked well in practice, despite the fact that it is undoubtedly unable to fully capture the flow dynamics specific to the nearby aquifer.

Infinite volume effect with a bulk volume of 10^3

The distribution of CO_2 saturation in the saline aquifer for a pore volume multiplier of 10^3 imposed to the boundary grids blocks is shown in Figure 5. Results shows a longer horizontal migration of supercritical CO_2 because of the rise in the pore volume of the boundary blocks. Gas saturation at the advancing front was 0.4883134 in grid block 89 1 1 at a distance of 884ft.

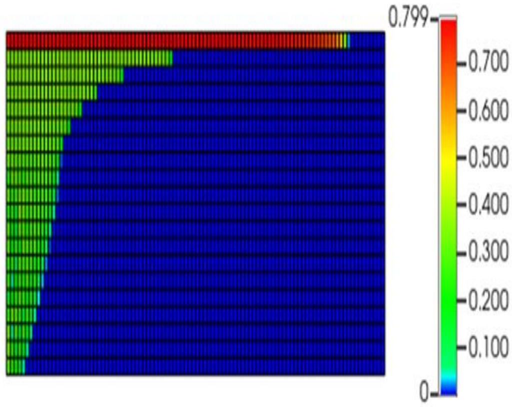

Figure 5 CO_2 saturation distribution for pore volume of 10^3

The amount of CO_2 trapped after 200years for a boundary block pore volume of 10^3 is presented in figure 6. The results indicate a continuous rise in the volume of trapped CO_2 over the injection period, attributed to the increasing pressure from the injection well and its impact on driving migration into the surrounding pore space. Over this specific period, a total of 16,570,669 moles of CO_2 was sequestered. Following the injection phase, the trapped amount of CO_2 significantly escalates due to the plume's upward and lateral movement driven by natural buoyancy and imbibition, reaching a total of 88,120,568 moles over the 199-year duration.

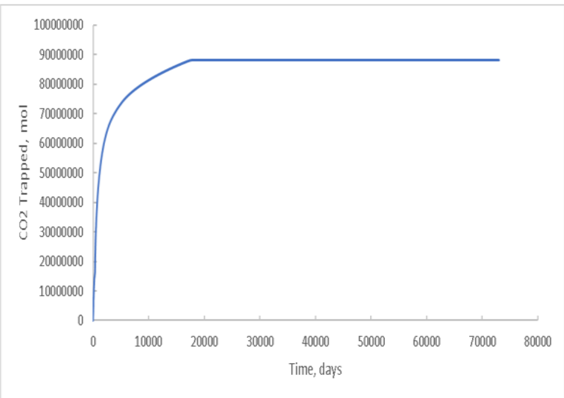

Figure 6 CO_2 trapped for bulk volume of 10^3

Infinite volume effect with bulk volume of 10^4

Figure 7 demonstrates the CO_2 saturation distribution within the saline aquifer model when pore volumes of the boundary blocks were increased to 10^4.Results reveals a longer horizontal migration of CO_2 gas as caused by the rise in the pore volume of the boundary blocks. Also, supercritical CO_2 occupies the first two layer of the structure as oppose to the case with a pore volume multiplier of 10^3. The gas saturation at the advancing front was 0.766912 in grid block 99 1 1 at a distance of 985ft along the aquifer length.

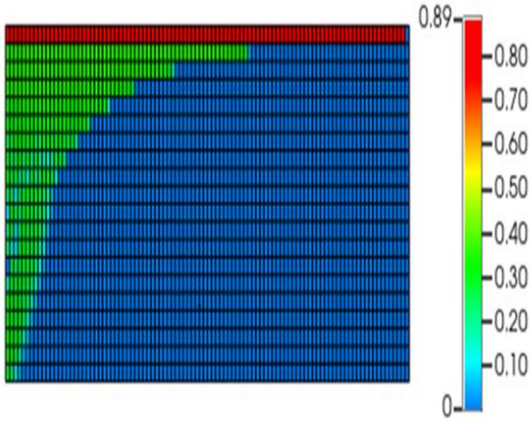

Figure 7 CO_2 trapped for bulk volume of 10^4

The quantity of CO_2 captured after 200 years of a boundary block pore volume of 10^4 is illustrated in figure 8. The results indicate a rise in the trapped CO_2 volume during the injection period, driven by heightened pressure from the injection well, influencing its migration into the surrounding formation's pores. This period witnessed the trapping of 18,451,372 moles of CO_2.

After injection, the quantity of trapped CO_2 significantly increases as the plume moves upwards and laterally due to natural buoyancy, reaching 96,803,000 moles over a 199-year span.

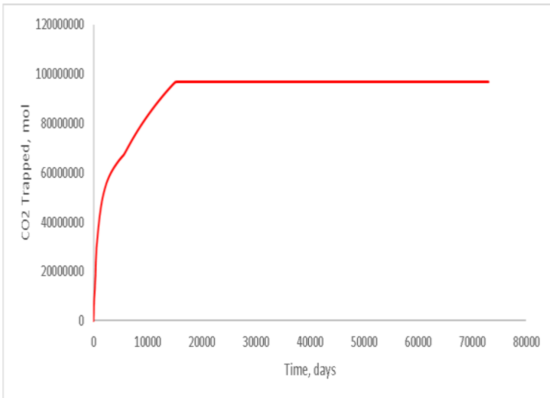

Figure 8 CO_2 trapped for bulk volume of 10^4.

Infinite volume effect bulk volume of 10^5

The distribution of CO_2 saturation in the saline aquifer model for pore volume of 10^5 is shown in figure in figure 9. Results shows an extensive horizontal migration of supercritical CO_2 gas as a result of the increase in the pore volume of the boundary blocks. The gas saturation at the advancing front was 0.7779648 in grid block 99 1 1 at a distance of 985ft along the aquifer length. When compared with the case for which the pore volume of the boundary blocks was 10^0, 10^3, 10^4, results reveal that for boundary blocks having a pore volume of 10^4 and 10^5, supercritical CO_2 migrated to the same distance along the aquifer boundary but with a different CO_2 saturation at the advancing front.

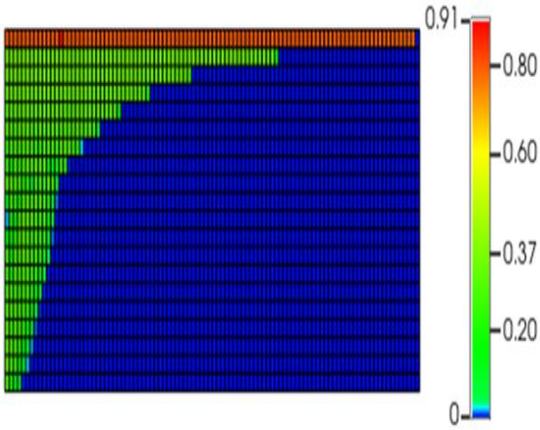

Figure 9 CO_2 trapped for bulk volume of 10^5

Figure 10 illustrate the amount of CO_2 trapped after 200years for a boundary block pore volume of 10^5. The findings indicate an escalation in the quantity of CO_2 trapped during the injection period as the injection well pressure propels its migration into the formation's pores. In this timeframe, 19305884 moles of CO_2 were confined. Following injection, the trapped CO_2 swiftly surges as the plume migrates upward and laterally due to natural buoyancy, totaling 101404776 moles over a 199-year duration.

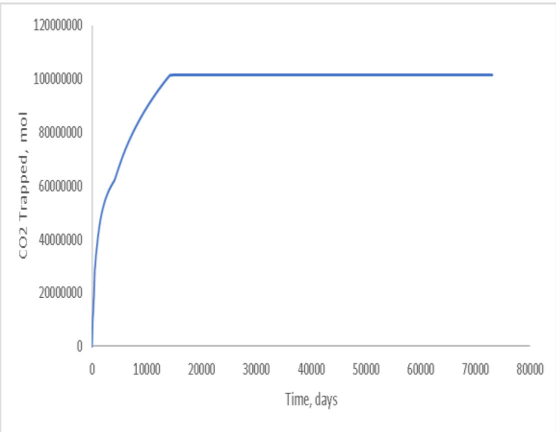

Figure 10 CO_2 trapped for pore volume of 10^5.

Comparison of base case with finite volume and infinite volume cases

Base case saline aquifer model with finite volume was compared with that of infinite extent to assess its contribution to CO_2-trapping enhancement. Results from base case model without accounting for infinite volume effect and that from models with infinite volume effect demonstrated that models with infinite volume effect resulted a higher amount of trapped CO_2 than the one with finite volume. Figure 11 highlights the extent of CO_2 trapped for the models with finite and infinite boundary blocks. Results depict an increase in the CO_2 trapped as the pore volume of the boundary blocks was elevated from 10^0 (base case) to 10^3, 10^4, and 10^5. The observed values were 59502924 moles for the base case study, 88120568 moles, 96803000 moles, and 1014047776 moles for the pore volume multipliers of 10^3, 10^4, and 10^5, correspondingly. This is due to the open aquifer that permits the brine to exit the system while maintaining a little pressure increase at the boundary.

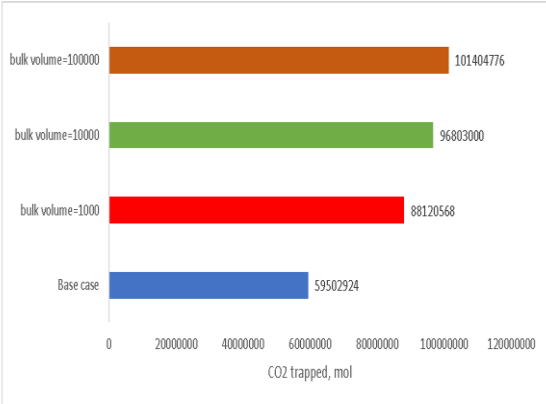

Figure 21 Comparison of CO_2 trapped for different aquifer sizes

Authors should discuss the results and how they can be interpreted in perspective of previous studies and of the working hypotheses. The findings and their implications should be discussed in the broadest context possible. Future research directions may also be highlighted.

Conclusions

CO_2 injection in a saline aquifer was simulated with emphasis on structural trapping mechanisms in an open aquifer that would immobilize (store) the CO_2. The flow of two components (CO_2 and H_2O) was simulated using a compositional simulator (CMG-GEM). A fluid model was established with the PR 1978 equation of state using WINPROP software. A finite aquifer model was built and compared with cases in which the aquifer was infinite (open). A number of simulation runs were conducted for three different cases with aquifer boundary block multiplied with a pore volume of 10^3, 10^4, and 10^5 to investigate the effect of open aquifer boundary on trapped gas saturation and CO_2 storage performance. For each these scenarios, the vertical CO_2 plume movement and the amount of trapped CO_2 over a time frame of 200 years after CO_2 injection has ceased were compared and the following conclusion drawn:

i. There was an increase in the quantity of trapped CO_2 as the pore volume of the boundary blocks increased.

ii. The moles of trapped CO_2 were almost constant after 20000 days for all pore volume scenarios.

iii. There was higher amount of trapped CO_2 for infinite volume than the finite volume.

iv. Lateral migration distance increased with increase in pore volume.

Funding Sources

This research did not received any external funding. It was basically done by the authors.

Conflicts of Interest

There was no conflict of interest.

Acknowledgements

We sincerely acknowledge the Department of Petroleum Engineering in Rivers State University and all individuals who played a part in the accomplishment of this research project.

References

[1] Ajayi, T., Gomes, J.S., & Bera, A. (2019). A review of CO2 storage in geological formations emphasizing modeling, monitoring and capacity estimation approaches. *Petroleum Science*, 16, 1028–1063. https://doi.org/10.1007/s12182-019-0340-8

[2] Amadichuku, N., Kinate, B.B., Isidore, E.A., & Epelle, S.I. (2023). The Impact of Relative Permeability Hysteresis on CO2 Sequestration in Saline Aquifer. *Current Trends in Engineering Science*, 3(2), 1026. https://doi.org/10.54026/CTES/1026

[3] Anchliya, A. (2009). *Aquifer Management for CO2 Sequestration*. College Station, Texas: Texas A&M University.

[4] Anchliya, A., Ehlig-Economides, C., & Jafarpour, B. (2012). Aquifer management to accelerate CO2 dissolution and trapping. *Society of Petroleum Engineers Journal*, 17, 805-816.

[5] Buscheck, T.A., Sun, Y., Chen, M., Hao, Y., Wolery, T.J., Bourcier, W.L., Court, B., Celia, M.A., Friedmann, S.J., & Aines, R.D. (2012). Active CO2 Reservoir Management for Carbon Storage: Analysis of Operational Strategies to Relieve Pressure Build-up and Improve Injectivity. *International Journal of Greenhouse Gas Control*, 6, 230−245.

[6] Ehlig-Economides, C., & Economides, M.J. (2010). Sequestering carbon dioxide in a closed underground volume. *Journal of Petroleum Science and Engineering*, 70, 123–130.

[7] Guo, F., Aryana, S.A., Wang, Y., McLaughlin, J.F., & Coddington, K. (2019). Enhancement of storage capacity of CO2 in megaporous saline aquifers using nanoparticle-stabilized CO2 foam. *International Journal of Greenhouse Gas Control*, 87, 134–141. https://doi.org/10.1016/j.ijggc.2019.05.024

[8] Han, S., Sang, S., Zhang, J., Xiang, W., & Ao, X. (2023). Assessment of CO2 geological storage capacity based on adsorption isothermal experiments at various temperatures: A case study of No. 3 coal in the Qinshui Basin. *Petroleum*, 9(2), 274–284. https://doi.org/10.1016/j.petlm.2022.04.001

[9] Kelemen, P.B., Benson, S.M., Pilorgé, H., Psarras, P., & Wilcox, J. (2019). An overview of the status and challenges of CO2 storage in minerals and geological formations. *Frontiers in Climate*, 1. https://doi.org/10.3389/fclim.2019.00009

[10] Li, Q., Wei, Y., Liu, G., & Lin, Q. (2014). Combination of CO2 geological storage with deep saline water recovery in western China: insights from numerical analyses. *Applied Energy*, 116, 101-110.

[11]Schembre-McCabe, J.M., Kamath, J., & Gurton, R. (2007). Mechanistic studies of CO2 sequestration. Paper IPTC 11391 presented at International Petroleum Technology Conference, Dubai, UAE.

[12] Van der Meer, L.G.H. (1995). The CO2 Storage Efficiency of Aquifers. *Energy Conversion and Management*, 36(6−9), 513−518.

[13] Van der Meer, L., & van Wees, J. (2006). Limitations to Storage Pressure in Finite Saline Aquifers and the Effect of CO2 Solubility on Storage Pressure. SPE Annual Technical Conference and Exhibition. San Antonio: Society of Petroleum Engineers.

[14] Van Engelenburg, B.A. (1993). Disposal of Carbon Dioxide in Permeable Underground Layers: A Feasible Option? *Climatic Change*, 55-69.

[15] Wei, N., Li, X., Jiao, Z., Stauffer, P.H., Liu, S., Ellett, K., & Middleton, R.S. (2022). A hierarchical framework for CO2 storage capacity in deep saline aquifer formations. *Frontiers in Earth Science*, 9. https://doi.org/10.3389/feart.2021.777323

[16] Yu, X., Catanescu, C.O., Bird, R.E., Satagopan, S., Baum, Z.J., Díaz, L.L., & Zhou, Q. (2023). Trends in Research and Development for CO2 Capture and Sequestration. *ACS Omega*, 8(13), 11643–11664. https://doi.org/10.1021/acsomega.2c05070